

NBSIR 76-1116

STABLE PRESSURE TRANSDUCER

Jack H. Colwell

Institute for Basic Standards
National Bureau of Standards
Department of Commerce
Washington, D. C. 20234

July 1976

Final Report

Prepared for

Aerospace Guidance and Metrology Center
Newark Air Force Station
Newark, Ohio 43055

CCG/Army/Navy
US Army Missile Command
US Army Metrology and Calibration Center
Redstone Arsenal, AL 35809

Naval Plant Representative
Metrology Engineering Center
1675 W. Mission Boulevard
Pomona, California 91766

ABSTRACT

This report describes the work done on the development of a solid-dielectric capacitive pressure transducer that is to have the accuracy and long term stability of which a piston gauge is capable. The temperature and pressure dependences of nearly one hundred samples have been measured in the process of trying to find materials for capacitors that would be capable of giving the requisite pressure resolution but not require excessively elaborate thermostating. To minimize temperature effects a technique has been developed whereby the ratio of two capacitors, made from different materials, is determined. By the proper choice of materials the temperature dependence of the ratio can be made small while the pressure dependence remains large. Two pairs of samples have been found which come close to meeting our requirements, the parallel and perpendicular cuts of calcite and a $\text{Bi}_{12}\text{GeO}_{20}$ (BGO) - As_2S_3 combination. The latter combination has the best potential for use in the transducer but samples of BGO have not been found which form stable capacitors. The system uses an Invar sample holder in a commercial pressure vessel and is designed so that it minimizes adiabatic heating effects and thereby shortens thermal equilibration times and simplifies thermostating. A limited-range automatic capacitance bridge has been built for use with the pressure transducer.

Key Words: Adiabatic Heating; Automatic Bridge; As_2S_3 ; $\text{Bi}_{12}\text{GeO}_{20}$; CaCO_3 ;
 CaF_2 ; Capacitance measurement; Evaporated electrodes; Pressure
Transducer

INTRODUCTION

Piston gauges have long been used for high precision pressure determinations and as transfer standards in the dissemination of pressure scales. These gauges are not simple to use, however, and should more properly be considered as devices for generating known pressures rather than as devices for measuring pressures. The cross-float procedure required to compare two piston gauges is very tedious. At high pressures, the use of piston gauges becomes awkward because of the large weights involved and because of the critical requirements placed on the selection of pressurizing fluids. In addition, quality piston gauges are expensive.

It would be very advantageous for precision pressure measurements if a direct-reading pressure transducer could be found which would possess the accuracy and long-term stability of the piston gauge. We set out to find a device meeting these requirements and, in addition, to seek one having the capability of digital readout and possibly automatic balancing. After a critical review of both existing and proposed pressure measuring devices we decided to try to develop a capacitive transducer in which the change in capacitance under hydrostatic pressure of a solid dielectric capacitor would be measured. The advantage of the dielectric capacitor over other devices is that using a hard, preferably crystalline, dielectric material with electrodes deposited directly on its surface, one would expect no permanent deformation to occur under repeated cycling with hydrostatic pressure and, therefore, to achieve the required long-term stability.

At the time this work was being initiated, Andeen, Fontanella, and Schuele (Rev. Sci. Instr. 42, 495 (1971)) of Case-Western Reserve University were demonstrating the feasibility of such a gauge using single crystals of

CaF₂ as a dielectric medium. With a CaF₂ capacitor, the capacitance changes only 0.26% when pressurized to 70 MPa (10,000 psi) so that the capacitance must be measured to $2.6:10^7$ in order to determine pressures to a precision of $1:10^4$ at 70 MPa. Using the three terminal capacitor method, modern A.C. bridge techniques, and accurate ratio transformers, capacitance measurements can be measured with accuracies of $1:10^7$ and with resolution of $1:10^8$. Piston gauges at 70 MPa have accuracies of about $1:10^5$ which is within the range of accuracy achievable with a CaF₂ capacitor. Tests have not indicated any instabilities in the capacitors so a gauge using a CaF₂ crystal does approach the basic pressure requirements. The capacitance of the CaF₂ gauge is, however, strongly temperature dependent; 1 mK changes the capacitance $2.6:10^7$, i.e., 1 mK would change a pressure determination at 70 MPa by $1:10^4$. Therefore, use of this gauge at the $1:10^5$ level would require that its temperature be maintained to much better than 1 mK. Thermostating to this level is clearly impractical, especially when one considers the heat generated in the pressure vessel whenever the pressure is changed and the long time required to reestablish thermal equilibrium.

As a result, a search was begun for materials which would have a greatly improved ratio of their pressure to temperature coefficients. Pyrolytic BN and As₂S₃ were found to be more than a factor of ten better than CaF₂ but this does not sufficiently alleviate the thermostating problem. As an expedient toward getting a working device, we began looking at other ways of overcoming the temperature dependence of the capacitance measurement. The bridge method required for the capacitance measurement offered ways of accomplishing this. One technique was to put capacitors of the same material in the opposite arms of the Wheatstone bridge circuit so that their capacitances are in opposition to each other. If one capacitor is pressurized and the

other kept at ambient pressure while keeping the two capacitors in thermal contact, the temperature will be cancelled to first order. James Miller of the U.S. Army Missile Command, Redstone Arsenal, has been pursuing developments along this line. The principal difficulty with this approach is that it requires the establishment of good thermal contact between a sample inside the pressure vessel and one outside. In our laboratory, we decided to concentrate on a variation of this same idea: placing in opposite arms of the bridge, two capacitors which have nearly equal temperature dependences but widely differing pressure dependences and placing both capacitors inside the pressure vessel. In this way, the temperature dependence of the combination could be largely cancelled out while retaining a reasonable pressure dependence but, with the two capacitors in close proximity to each other, thermal equilibration problems are eliminated. In pursuing this course, we have found only two combinations of materials which meet our requirements as far as temperature and pressure dependences are concerned, but both combinations turn out to be less than ideal as transducer materials for other reasons.

We are proceeding with the construction of a transducer based on this idea in the hope that these materials can be satisfactorily utilized or that other suitable combinations of materials may be found.

CAPACITANCE MEASUREMENTS

Capacitance Bridge. A schematic of the capacitance bridge used for these measurements is shown in Fig. 1. The main transformer was hand wound on a supermalloy toroid. The primary is shielded from the secondaries with a separate electrostatic shield and a heavy mu-metal shield. The main secondary is center tapped with a 10:1 turns ratio, the low impedance winding having a resistance of about 20 milliohms. A second set of center tapped secondaries with a 1:1 turns ratio is used with the quadrature balance circuit. The bridge is powered by a General Radio 1311-A audio oscillator operating at $\omega=10^4$ (1592 Hz).

The standard capacitors are 100 and 1000 pF General Radio type 1404 capacitors. By placing the appropriate capacitor on the appropriate side of the 10:1 transformer a full range of 10, 100, 1000, or 10,000 pF can be obtained. The standard capacitors are maintained in temperature controlled enclosure that is regulated to a few millikelvins.

The ratio transformers are a Gertsch model 1011 for the capacitance balance and a Gertsch RT 60 for the quadrature balance. The "phase splitter" circuit use for the quadrature phase shifter provides several different ranges of quadrature balance. Two resistors with nominal values of 10^5 and 10^6 ohms have been specially tuned to be pure resistances at $\omega=10^4$. With one of these resistors in the bridge circuit the phase shifter can be aligned by nulling the capacitive component.

The bridge null detector is a Princeton Applied Research model 120 lock-in detector with a model 112 preamplifier. The bridge imbalance is monitored with a chart recorder. At a bridge voltage of 70 v.p.p. the bridge resolution is 0.01 ppm.

Sample Preparation. The deposition of metallic electrodes on the dielectric samples has been the most difficult and time consuming problem throughout this work, both from the standpoint of forming the insulating gaps for the guard electrodes and because of poor adherence of the electrodes to the samples.

To properly utilize the three-terminal capacitance technique in a parallel-plate configuration, the low-voltage electrode should be considerably smaller than the high-voltage electrode (the difference in the radii of the electrodes should be at least three times the thickness of the sample). Also, the gap between the low-voltage electrode and the concentric guard ring should be kept very small. These restrictions are to minimize the fringing fields so that materials outside the dielectric sample will have little influence on the capacitance measurement.

The usual electrode configuration used for three-terminal capacitors is to have the high-voltage electrode cover one side of the sample, the low-voltage electrode and its surrounding guard ring cover the other side, and the edge of the sample left uncoated. We have modified the configuration as shown in Fig. 2, where the guard ring is coated around the edge of the sample with a separate gap left between it and the high-voltage electrode. This arrangement assures that the high-voltage electrode cannot electrically short to the side walls of the sample holders.

The metal electrodes are applied by vapor deposition and the gaps formed by masking. The masking rings were ground from hardened steel (both Hampden and Stentor 02 have been used) and the sharp edges were then lapped flat using a fine alumina compound. The dimensions of the two rings which are used with 25mm diameter samples is shown in Fig. 2. The attraction between the steel rings and a small bar magnet is sufficient so that the samples and rings can be supported in the evaporator in the manner shown in Fig. 2. To eliminate shadowing by the

ring it is necessary to rotate the sample during the deposition process and to position the evaporation source at about a 45° angle to the plane of the sample. With this masking technique we have successfully obtained gaps around the low-voltage electrode as small as $6\mu\text{m}$ but to avoid failures we usually used rings which left gaps of about $15\mu\text{m}$. There is no need for the gap around the high-voltage electrode to be narrow so a much wider masking ring was used here. With smaller diameter samples, rings of 12.7mm and 8.9mm diameters have been used and with the smaller diameter rings proportionally smaller gap widths have been obtained. Because the samples are coated at a 45° angle to the source, it is necessary for the sample surfaces to be reasonably well polished and flat ("two waves" is adequate) to avoid gap failure. It has been possible on several occasions, however, to vaporize small bridges across gaps by applying a few tens of volts between the electrode and the guard ring.

We have been using aluminum coatings on nearly all our samples and in most cases getting good adherence. By good adherence we mean coatings which cannot be pulled off with Scotch tape. This was accomplished after considerable trial and error and achieved mainly by getting the samples extremely clean. The procedure used is to wash the samples with soap and water, rinse thoroughly with distilled water, alcohol, and Freon, and then ion bombard in the evaporator in a glow discharge of air for upwards to one hour prior to coating. The use of 99.999% aluminum wire also improved the coatings considerably over the coatings from lower purity wire.

There are still several materials on which we cannot get good adherence with aluminum. In most cases we can still get good capacitance data with long term stability so it may be that the Scotch tape test is too stringent.

Sample Holder. The sample holder used for the capacitance measurements is shown in schematic cross section in Fig. 3. It was designed to provide flexibility so that, with minor modification, samples of different diameter or thickness could be run. The center piece has a shoulder on which the guard ring of the sample rests. The two end pieces are of identical construction and hold the electrical contacts. The electrical contacts are small gold-plated nickel-deposited bellows, which are 3mm in diameter, 5mm long and can be compressed up to 1.8mm. The advantage in using the bellows is that their spring constants are very consistent (90g/mm) so that the force on the contacts can be predetermined by adjusting the amount that the bellows will be compressed when the sample holder is assembled. This adjustment is made by varying the thickness of the Teflon washers which insulate the contacts from the body of the sample holder. The bellows of the high-voltage contact is usually compressed 1mm (90g load) and that of the low voltage contact 0.5mm (45g load). In this way, there is sufficient load (45g) on the sample to ensure that good electrical contact between the guard ring of the sample and the grounded case of sample holder is maintained. With this arrangement, we have had no trouble with contacts opening during pressure cycling.

Five sample holders can be mounted on screw rods extending from the bottom of the pressure vessel closure as shown in Fig. 4. The high-voltage contacts are connected by miniature coaxial cables to a connector plate on the bottom side of the closure. The electrical feed-throughs are connected to the contacts on the reverse side of this plate. The low voltage contacts from the five cells are interconnected and brought out of the vessel by a single lead which is carefully shielded from the others.

Pressure System. The pressure vessel used for this work has an internal diameter of 3.8 cm (1.5 in.), has an internal length of 25cm (10 in.), and is rated for 138 MPa (20,000 psi). The vessel has an opening in the bottom which was used for the pressure connection. The closure was modified with four openings to accept three shielded twin-ax and one coax feedthrough (P.L.M. Heydemann, Rev. Sci. Instr. 38-550 (1967)). Subsequently, one of the twin-ax feedthroughs was replaced by a pressure connection, so that the pressurizing oil could be forced in from the bottom of the vessel and out through the top thereby purging the air from the system. This arrangement permitted the use of only four samples at a time but it had been suspected that air bubbles were causing some irreproducibility in the zero pressure capacitance reading.

Pressures are generated by an air operated pump which compresses oil from a reservoir into a large pressure vessel which serves as a buffer to smooth out pump strokes. The buffer vessel is valved directly to the research pressure vessel. Pressures are measured with a 276 MPa Heise Bourdon-tube gauge which is connected directly to the pressure vessel. This gauge is accurate enough (0.3% of full scale) for determining pressure coefficients but for more accurate pressure measurements a Ruska type 2415, 0-138 MPa piston gauge has been used.

The pressure system was initially filled with instrument oil but this had to be removed when it became contaminated with moisture. The system was subsequently filled with paraffin oil which was found to have a much higher resistivity than other oils even after long exposure to the atmosphere, $\rho \approx 5 \times 10^{11} \Omega$.

Thermostat and Temperature Measurement. To thermostat the pressure vessel it was immersed in a large, insulated, water-glycol bath. Fluid from a

liquid thermostat is pumped into the bath at the bottom and led back to the thermostat from the top. A refrigerator circulates methanol at -20°C through the cooling coils of the thermostat. A heater, controlled by a contact thermometer, maintains a set temperature in the thermostat fluid. The temperature of the pressure vessel is measured with a platinum resistance thermometer. The thermometer is in a brass block which is in good thermal contact with the pressure vessel. The temperature of the pressure vessel can be regulated at any point between 0 and 50°C to within 5mK for a period of hours and within 20 mK for several weeks. The resistance of the platinum thermometer is measured with Leeds and Northrup, 8069-B Mueller Temperature Bridge which is operated at 27Hz rather than at DC as intended. By using AC, the bridge imbalance could be determined with a phase-sensitive detector and recorded on a chart recorder. Using AC, there is no need for lead reversals to eliminate "thermals." We ran many comparisons between AC and DC measurements and, within the bridge resolution ($\pm 0.1\text{mK}$), could find no differences. Presumably, 27 Hz is a low enough frequency that inductive effects in the Mueller bridge are negligible.

CAPACITANCE DATA

We have looked at over one hundred samples during the progress of this work. In Table 1, we bring together the temperature and pressure dependences of the capacitance for most of the different materials studied. Much of these data are plotted in Fig. 6 together with data by other investigators on several other materials. The lines joining the values for the two orientations of anisotropic materials indicated all the values that could be obtained with samples of intermediate orientations. As can be seen in Fig. 6, most materials fall into the quadrant of positive temperature coefficients and negative pressure coefficients. This is as one might intuitively expect for the pressure dependence, i.e., the material is less polarizable at smaller volumes, but the temperature dependence is not easily explained. There are a reasonably large group of materials (not shown) with both coefficients negative. These are the paraelectrics of which the thallous halides are examples. For these, both the temperature and pressure dependences follow a Curie-Weiss type relation and are usually rather large. The unifying characteristic of all the materials with positive pressure coefficients is that they are all anisotropic. The As_2S_3 samples are actually glasses, but crystalline As_2S_3 is very anisotropic.

The majority of the materials were, for our purposes, well behaved, i.e., the measured capacitances did not drift, the loss components were small, and electrodes adhered well. There are specific classes of materials which do not behave well: they are piezoelectric and pyroelectric crystals, ceramics, and impure materials.

Table I Capacitance Data

Material	Dielectric Constant	$\frac{1}{C} \frac{dC}{dP} \times 10^{12}/\text{Pa}$	$\frac{1}{C} \frac{dC}{dT} \times 10^6/\text{K}$
CaF ₂	6.8	-37.6	262.7
TlCl	31.4	-212	-355
TlBr	30.3	-220	-320
KRS-5	32.0	-245	-470
BN, Pyrolytic	3.4	121	-51
BN, Hot Pressed	4.5	62	140
Quartz			
X-cut	4.5	7.7	-2.4
Y-cut	4.5	7.7	-3.5
Z-cut	4.7	-1.9	33.4
XLZ 45°	4.6	7.7	10.4
YLX 45°	4.6	2.8	20.4
Sapphire			
(0001)	11.5	-11.6	136.3
(10 $\bar{1}$ 0)	9.4	-10.6	95.8
(1120)	9.5	-10.7	95.9
(1 $\bar{1}$ 02)	10.0	-10.6	107.8
Lucalox	10.2	-52.8	146
MgF ₂	5.5	-13.26	172.3
MgF ₂	4.8	-21.13	199.4
MgF ₂ Ceramic	5.3	-21.6	215
Irtran 1			
GGG(Gd ₃ Ga ₅ O ₁₂)	12.6	-17.0	127

Table I (continued)

Material	Dielectric Constant	$\frac{1}{C} \frac{dC}{dP} \times 10^{12}/\text{Pa}$	$\frac{1}{C} \frac{dC}{dT} \times 10^6/\text{K}$
As_2S_3			
(Servo)	7.4	116	63.5
"	7.7	113	78.3
"	7.8	110	75.4
(Barnes)	7.7	114	66.4
Spinel (MgAl_2O_4)	8.4	-12.5	135.3
Glass (NBS)	6.5	-22.5	139
Glass (UK50)	6.4	-34.3	236
Zirconate			
Ceramic	34.4	-51	16.8
Calcite	8.0	12.2	327.2
Calcite	7.7	72.0	329.0
$\text{CaF}_2\text{-3\%Er}^{3+}$	5.6	-50.4	182
LiTaO_3	54	-47.1	165.6
LiTaO_3	44	-27.7	1302.5
$\text{BGO}(\text{Bi}_{12}\text{GeO}_{20})$	46	-102.7	73.5
Diamond	5.9	- 1.444	9.2
TeO_2	23	22.8	151.0
TeO_2	27	- 38.0	255.5
LiNbO_3	83	- 59.1	387
LiNbO_3	29	- 6.8	734

The piezoelectric materials, quartz and BGO, both underwent long term relaxations after pressure changes. Quartz was particularly bad in this respect where large relaxations (40% of total change) were observed with relaxation times of the order of a day. This was only true for crystals with a component of the Z axis parallel to the electric field, the X and Y cuts were well behaved. It may be significant that strain cannot produce a polarization change along the Z axis in quartz, but this information does not lead to an obvious explanation. BGO has similar effects but they are much smaller in magnitude, this will be discuss more fully below.

LiNbO_3 and LiTaO_3 are pyroelectrics, i.e. polarized ferroelectrics. The samples were poled, single domain crystals cut parallel and perpendicular to the axis of polarization. All four crystals underwent rather large relaxations after temperature or pressure changes which went on for several hours. The niobates were some two orders of magnitude more lossy than our normal crystals, while the tanatalates were only about one order of magnitude larger.

The zirconate ceramic, Lucalox (Al_2O_3 ceramic), and hot pressed BN were both very lossy and drifted about continuously.

Impure MgF_2 samples had a large loss component and a pronounced relaxation in the capacitance. A poor quality BGO sample had much large relaxations than did better quality samples.

We have had trouble getting aluminum to adhere well to the thallium salts, BGO, and As_2S_3 .

We have carried out a detailed analysis of the temperature and pressure dependence of several samples which have shown promise for use in a transducer. Using a piston gauge for precise pressure determinations, measurements were made at four different temperatures so that the cross derivatives of the capacitance could be determined. The data were assumed to have the usual functional form

$$C = C^0 (1 + AP + BP^2) \quad (1)$$

which rearranges to

$$\frac{\Delta C}{PC^\circ} = A + BP. \quad (2)$$

Accordingly, with the data plotted as $\Delta C/(PC^\circ)$ versus P the quantities A and B are determined, respectively, by the intercept and slope of the lines. The plot for CaF_2 is shown as an example in Fig. 5. From these data dA/dT can be derived, this quantity is required to determine the temperature dependence of the pressure equation (Eq.1).

In Table 2 we have collected together data obtained in the above fashion which is exemplary and will serve our discussion below.

Table 2. Temperature and Pressure Characteristics of Capacitor.

Material	$\frac{1}{C^\circ} \frac{dC^\circ}{dT} \times 10^6/K$	$\frac{1}{C^\circ} \frac{dC^\circ}{dP} = A \times 10^{12}/\text{Pa}$	$\frac{dA}{dT} \times 10^{12}/(\text{PaK})$	$B \times 10^{20}/\text{Pa}^2$
CaF_2	263	-37.8	-0.025	0.27
$\text{CaCO}_3 \perp$	331.5	12.0	0.0149	0.42
$\text{CaCO}_3 \parallel$	335	71.0	0.0169	1.25
As_2S_3	76.7	110.6	0.030	-1.4
$\text{BGO}(\text{Bi}_{12}\text{GeO}_{20})$	73.7	-102.8	0.037	2.0

Table 3. Temperature and Pressure Characteristics of Pair Combinations.

Material	$\frac{1}{R^\circ} \frac{dR^\circ}{dT} \times 10^6/K$	$\frac{1}{R^\circ} \frac{dR^\circ}{dP} = A_r \times 10^{12}/\text{Pa}$	$\frac{dA_r}{dT} \times 10^{12}/(\text{PaK})$	$B_r \times 10^{20}/\text{Pa}^2$
CaCO_3 Pair	3.6	59.0	0.0020	0.76
$\text{BGO}-\text{As}_2\text{S}_3$	3	213.4	-0.007	-1.2

The typical behavior of the pressure equations is that the coefficients A and B have opposite signs, i.e. the capacitance changes less rapidly as the pressure increases. This is not true of CaCO_3 and this may in fact be an early indication the phase transition which occurs in this material at 1.4 GPa. For materials with positive temperature coefficients A and dA/dT have the same sign, except for BGO which appears to be unique in this respect.

PRESSURE RESOLUTION AND TEMPERATURE EFFECTS WITH CAPACITOR PAIR COMBINATIONS.

In our attempt at circumventing the temperature dependence inherent in individual dielectric capacitors, we have been using a device where two different capacitors, placed in opposite arms of the Wheatstone bridge measuring circuit are both within the pressure vessel. The resulting bridge balance gives the ratio of the two capacitance,

$$R = C_1/C_2 \quad (3)$$

The observed change of the ratio measurement as a function of temperature or pressure is

$$\frac{1}{R} \frac{dR}{dT} = \frac{1}{C_1} \frac{dC_1}{dT} - \frac{1}{C_2} \frac{dC_2}{dT} \quad (4)$$

and

$$\frac{1}{R} \frac{dR}{dP} = \frac{1}{C_1} \frac{dC_1}{dP} - \frac{1}{C_2} \frac{dC_2}{dP} \quad (5)$$

The appropriate capacitors combinations for use in this type of pressure transducer are therefore, ones having nearly identical temperature dependences but widely differing pressure dependences. It should be pointed out in Eq. 4 that it is the fractional temperature dependences of the capacitances that must be equated, this is a property of the material and does not depend on the size of the capacitance. What we need to find are pairs of materials, which in the plot in Fig. 6, are displaced from each other along a nearly vertical line, but are displaced by enough to give sufficient pressure resolution. Initially, no appropriate combinations were known and we began our search by looking at anisotropic materials. The capacitance along different axes in anisotropic materials are usually quite different and intermediate values can be obtained with samples cut at the various angles between the principle axes. This

approach did not directly produce any useful combinations but it did lead to the combination of parallel and perpendicular cuts of calcite (CaCO_3) which can be used as a pair in a pressure transducer. Subsequently a second useful combination was found which consists of $\text{Bi}_{12}\text{GeO}_{20}$ (BGO) and As_2S_3 .

The data on the capacitor pair combinations can be analysed in the same fashion as that of the individual capacitors given in Eq. 1 by writing

$$R = R^\circ (1 + A_r P + B_r P^2). \quad (6)$$

This can be evaluated directly or from the data on the individual capacitors C_1 and C_2 as defined by Eq. 1, since

$$R = \frac{C_1^\circ}{C_2^\circ} \left(1 + (A_1 - A_2) P + [(B_1 - B_2) - A_2(A_1 - A_2)] P^2 + \dots \right) \quad (7)$$

Similarly, the pressure and temperature derivatives of R leads to expressions involving the differences of the corresponding terms for the individual capacitors such as

$$\begin{aligned} \frac{1}{R} \frac{dR}{dT} &= \frac{1}{R^\circ} \frac{dR^\circ}{dT} + \frac{dA_r}{dT} P + \dots \\ &= \frac{1}{C_1^\circ} \frac{dC_1^\circ}{dT} - \frac{1}{C_2^\circ} \frac{dC_2^\circ}{dT} + \left(\frac{dA_1}{dT} - \frac{dA_2}{dT} \right) P + \dots \end{aligned} \quad (8)$$

and

$$\begin{aligned} \frac{1}{R} \frac{dR}{dP} &= A_r + (2B_r - A_r^2) P \\ &= (A_1 - A_2) - \left[2(B_1 - B_2) - (A_1^2 - A_2^2) \right] P + \dots \end{aligned} \quad (9)$$

Data for the calcite pair and the BGO- As_2S_3 combination are given in Table 3. The data obtained from the capacitor combinations agree with that derived from the individual measurements using Eqns. 7-9.

In the introduction we stated that the resolution of a piston gauge at pressures in the range of 70 MPa (10,000 psi) is about $1:10^5$ or 700 Pa (0.1 psi). To be able to measure a pressure change of 700 Pa with a calcite pair transducer requires that we be able to measure the fractional capacitance changes to the following level,

$$\frac{1}{R} \frac{dR}{dP} \times \Delta P = 59.0 \times 10^{-12}/\text{Pa} \times 700 \text{ Pa} = 4.2 \times 10^{-8}$$

This value is within the resolution of our bridge of $1:10^8$ but beyond the stated accuracies of bridge ratio transformers, $1:10^7$. Whether non-linearities in the bridge could be corrected for in the calibration procedure would have to be determined. It should be pointed out that the pressure resolution of the capacitance gauge is nearly independent of total pressure so that its fractional resolution, $\Delta P/P$, is better at higher pressures. With the piston gauge it is the fractional resolution which remains essentially constant except for the lower end of its range where its precision drops off.

The temperature stability and accuracy which is required enters in three different ways.

- (1) the two capacitors must be in thermal equilibrium with each other.

This depends not on the pressure dependence of the capacitor pair but on the temperature dependence of the individual capacitors (which by choice are nearly identical). The total temperature difference between a pair of calcite crystals that would be equivalent to a pressure change of 700 Pa is

$$\Delta T = \frac{\frac{1}{R} \frac{dR}{dP} \Delta P}{\frac{1}{C} \frac{dC}{dT}} = \frac{59.0 \times 10^{-12} \times 700}{333 \times 10^{-6}} = 0.12 \text{ mK.}$$

This is a small temperature difference but should be no difficulty since the two capacitors will be in close proximity and symmetrically located at the center of the pressure vessel.

- (2) The temperature of the capacitance pair for the determination of R under pressure must be the same as it was for the determination of R° at zero pressure. The allowable deviation of the temperature between these two measurements depends somewhat on the pressure measured. The temperature change that is equivalent to 700 Pa for a calcite pair is

$$\Delta T = \frac{\frac{1}{R} \frac{dR}{dP} \Delta P}{\frac{1}{R^\circ} \frac{dR^\circ}{dT} + \frac{dA_r}{dT} P} = \frac{59.0 \times 10^{-12} \times 700}{3.6 \times 10^{-6} + 0.002 \times 10^{-12} P} = 11.5 \rightarrow 11.0 \text{ mK}$$

Where the range of values is for pressures between zero and 70 MPa. Thus the temperature can change by several millikelvin during the pressure cycling and have no effect on the pressure resolution at the 700 Pa level.

- (3) The final temperature effect arises from the temperature dependence of the pressure coefficient and requires that the pressure transducer be operated at the temperature at which it was calibrated. The uncertainty in the absolute temperature or displacement therefrom which will cause an uncertainty of 700 Pa in a pressure determination of 70 MPa is

$$\Delta T = \frac{\frac{1}{R} \frac{dR}{dP} \Delta P}{\frac{dA}{dT} P} = \frac{59.0 \times 10^{-12} \times 700}{0.002 \times 10^{-12} \times 70 \times 10^6} = 295 \text{ mK.}$$

The inverse pressure dependence makes this restriction more stringent at high pressures.

These results show that a practical pressure transducer could be made from a pair of calcite capacitors. The pressure resolution may be considered marginal even though it is 50% greater than the CaF_2 transducer originally considered, but the thermal requirements are very reasonable and could be easily met. The real drawback is that the crystals are very fragile. The material is hard but it cleaves rather easily. We had no trouble with these crystals in our research apparatus, but in the prototype transducer (see below) we have repeatedly broken crystals. The problem appears to be due to poor oil flow through the sample holder which lifts the crystals off their contacts. The holder has been modified to correct this but not tested.

The temperature and pressure dependences of the $\text{BGO-As}_2\text{S}_3$ combination show it to have great potential. The pressure dependence is 3.6 times that of the calcite pair so that it should be possible to resolve 70 Pa (0.01 psi) with this pair and to have known accuracy at the 700 Pa (0.1 psi) level. The thermal requirements with the $\text{BGO-As}_2\text{S}_3$ combination are listed in Table 4 with those for the calcite pair. Comparison shows the large improvement that could be achieved with this combination.

Table 4. Thermal Stability Required to Obtain 700 Pa (0.1 psi)
Pressure Resolution with a Calcite Pair and a BGO -
 As_2S_3 Capacitor Combination.

<u>Materials</u>	<u>Thermal Equilibrium</u> <u>Between Capacitors</u>	<u>Short Term</u> <u>Temperature Stability</u>		<u>Long Term</u> <u>Temperature Accuracy</u>
		<u>At 0 Pa</u>	<u>At 70 MPa</u>	<u>At 70 MPa</u>
CaCO_3	0.12 mK	11.5 mK	11.0 mK	295 mK
$\text{BGO} - \text{As}_2\text{S}_3$	2.0 mK	50 mK	63 mK	305 mK

The drawback with the BGO-As₂S₃ combination is with the BGO crystals. This material is piezoelectric and as already mentioned, such materials have large relaxation effects after temperature or pressure changes the reason for which is not known. Our initial sample of this material was of poor quality, it was opaque, and showed large relaxations. A second set of samples were of much better quality and were optically clear. These crystals still showed relaxation effects, though much smaller than before and also showed some discontinuous effects. When samples were repeatedly pressure cycled to 140 MPa, the capacitance ratio would return to its zero value several times and then shift to a new value, displaced by upwards to the equivalent of 7000 Pa (1 psi). The shifts were nearly always in the same direction. When the cell was held at pressure for a period of time the capacitance would drift slowly to higher values, then when returned to zero it would relax back to its initial value over a period of hours.

We do not know the cause of this behavior, but we suspect it is due to crystalline imperfections, dislocations or possible impurities, causing strain in the crystals. This is important in piezoelectrics but not in ordinary crystals since the strains will effect the bulk polarization and therefore the polarizability. Because of the attractiveness of this material as a transducer we are purchasing more crystal, of presumably higher quality, to see if they will be better behaved. Crystals of three different orientations are going to be tested to see if there may be different behavior in the different directions as in quartz. This is not too likely since BGO is cubic and the piezoelectric constant is isotropic, but it is worth the effort since the cause of the problem is unknown. There is a possibility that the problem with BGO may be with the coating for we have not been able to get aluminum to adhere well to it. This is also true of As₂S₃ but we have found no adverse effects

with this material. During the more than one hundred pressure cycles the BGO-As₂S₃ combination was put through the As₂S₃ capacitance always returned to the same value.

Adiabatic Heating and Transducer Thermostating.

The simplest way to thermostat a system is to isolate it as well as possible from the surroundings and to minimize any disturbances that would tend to change its temperature. The thermostating of the pressure transducer is complicated, however, by the adiabatic heating effects which occur whenever the pressure is changed. When the pressure transducer is pressurized, all the material inside the pressure vessel (the samples, sample holder, and pressurizing oil) are under compressive stress and increase in temperature. The pressure vessel itself is placed under a net tensile stress when the pressure increases and, as a result, it cools. The reverse occurs when the transducer is depressurized. Consequently, in thermostating the transducer one would need, in general, the capability of both heating and cooling the system. Also, with part of the system warming and others cooling, a rapidly-responding thermostat would probably prolong the period of equilibration.

We have managed to get around this problem by equating the heating and cooling that occur within the transducer during any pressure change, so that there will be little or no temperature change when thermal equilibrium is reestablished.

The amount of heating that occurs in a piece of material under compressive or tensile stress is given by

$$Q = TV\bar{\beta}\Delta P,$$

where $\bar{\beta}$ is the average thermal expansion coefficient for the range of the pressure change, ΔP , and \bar{V} is the average volume.

The cooling that occurs in the pressure vessel itself (see Appendix), when it is internally pressurized, is equal in magnitude to the amount of heating that would occur upon externally pressurizing a piece of steel of the same composition as that of the vessel and having the same volume as the internal volume of the vessel. In other words, if we could completely fill the inside of the vessel with a steel plug and then pressurize the system using a negligibly small amount of oil, there would be no temperature change when equilibrium is reestablished.

For steels such as that of the pressure vessel, the thermal expansion coefficient is about 55 in units of $10^{-6}/K$. The paraffin oil we have been using as a pressurizing fluid has a coefficient of about 750. Since we must have at least a small quantity of oil in the transducer, we need to offset its large coefficient by including in the pressure vessel a large amount of material with a thermal expansion coefficient smaller than steel. Fortunately, there is a suitable material, Invar, a high nickel steel, that has a thermal expansion coefficient of only 3.6 units. By limiting the volume of oil in the pressure vessel to about 7% of the total volume (12 cm^3) and filling the rest of available volume with Invar, we calculate that temperature changes can be kept at a negligible level. The heating effects cannot be eliminated completely because the oil is highly compressible so that its expansion is a marked function of the pressure.

For the prototype pressure transducer we are using a commercial (High Pressure Equipment Company) pressure vessel with a pressure rating of 138 MPa (20,000 psi). The vessel has a 3.8 cm (1.5 in.) I.D. and a depth of 15 cm (6 in.) and comes with a pressure connection in the bottom of the vessel and one in the center of the one-piece threaded closure. We have modified the closure with three additional pressure connections to allow for the separate entry of the three electrical feed-throughs required for the capacitance measurements.

An Invar sample holder has been fabricated which attaches to the bottom of the pressure closure and effectively fills the entire volume of the pressure vessel. The sample holder, diagramed in Fig. 7, was made from six 6.3 mm ($\frac{1}{4}$ in.) plates, which, when bolted together, form the cylindrical plug shown on the left. The central two pieces hold the low voltage electrode, which is common to both capacitors, and the capacitors themselves fit into recesses on the outside of these pieces. The next two pieces hold the high voltage electrodes, which make contact with the back of the capacitors. The three electrodes are made from small gold-deposited bellows, the same as used in our experimental system. The position of two outer electrodes can be adjusted to ensure sufficient force on the contacts for electrical continuity. The outer two plates simply fill out the volume. A picture of the partially disassembled sample holder is shown with the pressure vessel in Fig. 8.

Our experiments indicate that the ideas incorporated in this device are basically correct. In Fig. 9 we show the actual temperature change observed with the system upon changing the pressure. The pressure vessel was effectively isolated from the surroundings in an insulated container with a thermometer attached to the outer surface of the pressure vessel. At the center of the figure is shown the effect of depressurizing the vessel over about a 1 minute period from 140 MPa (20,000 psi) to zero. The outer surface of the vessel first warms, but as the vessel thermally equilibrates with the material inside, it cools, stopping at a temperature 4 mK below the initial temperature. To the right is seen the reverse effect when the system was repressurized. The slope of the base line in the figure is due to the small loss of heat to the surroundings. We calculate that each cm^3 of oil in the system that is displaced by invar will produce a 3 mK difference in the temperature change observed with a 140 MPa pressure change. The results in Fig. 9 indicate that $1\frac{1}{3} \text{ cm}^3$ more oil needs to be displaced from the system to exactly balance the heating and cooling effects. To get to this

point it was necessary to displace much more oil than predicted by the calculation. In Fig. 10 we have plotted the temperature changes observed with three different quantities of oil in the system and find that the temperature changes are varying as predicted but are displaced from the calculated curve by nearly 8 cm^3 of oil. Although it is not easy to determine the exact amount of oil in the system, (considering screw slots, counter sinks, oil equivalent of the O-ring seal, etc.) we do not think we are in error by this amount. The volume differences between the plotted points in Fig. 10 are accurately known, however, for they were determined by the volume of the invar pieces used to displace successive quantities of oil. A possible cause of the discrepancy is our failure to properly account for the heating effects of the threaded vessel closure; our calculation assumed that the vessel has spherical ends. A more likely cause is that the expansivity values we used for the materials involved are badly in error. This is unfortunate for in designing the sample holder we were overgenerous in the size of the openings allowed for various purposes and the pieces will be difficult to modify.

We have shown earlier that for the capacitor combinations (calcite-pair or BGO-As₂S₃ combination) we are considering, the change in temperature which can be tolerated at different pressures is in excess of 10mK. With the Invar sample holder the changes in temperature that occur when the pressure is changed will be considerably less than that value. As a result, there is no need to actively thermostat the pressure vessel itself, but to thermostat only its surroundings so that the temperature of the vessel stays within prescribed bounds.

The thermostating arrangement to be used will consist of placing the pressure vessel in a highly conductive container but insulating the vessel from the container so that the thermal relaxation time will be tens of minutes. The container itself will then be well insulated from the surrounding and regulated at about 35°C , well above room temperature. Since the conductive container will be well

insulated from all disturbances its regulator can be rather unsophisticated. The pressure vessel will require a separate thermometer to assure that it is within the prescribed temperature range as well as an auxiliary heater to bring it initially to the thermostated temperature.

AUTOMATIC CAPACITANCE BRIDGE

A limited-range capacitance bridge has been constructed which was designed specifically for use with the dielectric capacitance pressure gauge. It is capable of measuring the ratio of two capacitors which differ by less than 10% and which also have reasonably small loss tangents. After an initial adjustment, the bridge operation is completely automatic.

The design of the bridge proper, shown in Fig. 11, is in principle the same as that being used as a research tool in our laboratory. The bridge transformer forms the 1:1 ratio arm of the bridge and supplies the voltage for the ratio transformer used in balancing the bridge. The output voltage of the ratio transformer is injected into one of the ratio arms of the bridge through the two stage transformer. The power for this injected voltage comes from an operational amplifier so that there is no loading of the ratio transformer and the bridge impedance is kept small. It is the turns ratio on the two stage transformer and the voltage supplied to the ratio transformer that limits the range of capacitor ratios that can be measured. A switch on the primary of the two stage transformer allows the selection of a total range of either 1 or 10%. The switch on the input to the ratio transformer allows this range of bridge ratios to be taken on either the positive or negative sides or centered about the ratio of 1. Any difference in loss between the measuring capacitor and the reference capacitor is compensated by injecting an in-phase, i.e. resistive component, signal into the detector arm of the bridge. The magnitude of this signal is controlled by multiplying the D.C. in-phase signal of the phase sensitive detector by an A.C. signal from the bridge transformer.

Fig. 12 is a block diagram of the logic circuitry for the automation of the capacitance bridge. The design was limited to some extent by the incorporation of a 5 decade programmable ratio transformer (PRT). We require a 7 digit reading

and would desire 8 digits, so it is necessary to limit the range of capacitance ratios that the instrument can cover. In the 1% range the first two significant digits are preset by the range control, in the 10% range only the first significant digits are determined by the ratio transformer and two additional digits are obtained by the digital conversion of the analog voltage resulting from any remaining bridge imbalance.

In operation the imbalance current from the capacitance bridge is amplified by an FET preamplifier and by three programmable gain amplifier sections. The FET preamplifier goes directly on the pressure transducer thereby reducing the effects of lead capacitance on the bridge. These are followed by two lock-in amplifiers, one phased to detect the resistive loss component of the bridge and the other phased at 90° to detect the capacitive imbalance. The rectified loss component is further filtered and used to control the automatic loss feedback network in the bridge. This signal can be monitored through a front panel BNC connector.

The rectified capacitance imbalance signal is fed to the gain control module and to two voltage-to-frequency converters (VFC). The signal is inverted before one of the VFC, so that one VFC delivers a pulse rate proportional to positive signals and the other to negative signals.

The output of the two VFC's are fed into a bank of 14 up-down counters by way of a multiplex unit that switches in and out various counters. After each period of counting the contents of the counters are dumped into latches which hold that count while the next is in progress. The signals from the latches are routed through buffers to the BCD output for external processing and are routed to the seven-segment decoders which generate a 10 digit seven-segment incandescent display. The signal from latches 4', 5, 6, 7, and 8 are routed through drivers to the programmable ratio transformer and provide the updated bridge setting. Only decades 9 through 13 are zeroed before each count so that

the new count is added to or subtracted from the existing transformer setting.

The clock steps down the bridge frequency to approximately 10 second and 1 second intervals which are used as counting times. The clock is used to turn the counters on and off, and while the counters are off enables the gain control and range control, transfers information from the decade counter to the latches, zeros counters 9 through 13 and turns on the counters for the next interval.

The gain control looks at the output of the bridge and sets the amplifier gain decades to keep the input to the VFC's less than 10 volts but greater than 1/2 volt. It is operative only when the counters are off. When the amplifier gain changes the counting gain or count time must change to keep the overall gain constant. The counter gain is changed by the multiplexers switching between the last five decade counters. On the highest amplifier gain the clock is set for 10 second counts; on all other gains it is set for 1 second counts.

The range control switches between the following deviation capabilities of the bridge: 0 to 1%, $\pm 1/2\%$, -1 to 0%, 0 to 10%, $\pm 5\%$, and -10 to 0%. The switching is done automatically seeking the highest sensitivity. Range control switching takes place only when the counter is off and only when the programmable ratio transformer is asked to go beyond its limit (as detected by a carry or borrow signal from counter 4'). Counters 1, 2, 3, 4, 4' are reset each time a range control switching occurs.

Decade counters 9 and 10 do not control the bridge. They are zeroed before each count and provide the two analog decades of bridge sensitivity beyond the ratio transformer setting.

The fourth decade is split, 4 going to the readout and 4' controlling the PRT. This was necessary to permit the use of the bridge ranges $\pm 1/2\%$ and $\pm 5\%$. On these ranges, when the bridge ratio (and readout) is exactly 1.000, the PRT must be set to 50000, the 5 appearing in the fourth readout decade.

The precision desired from this bridge, $1:10^7$, is pushing the limits of the programmable ratio transformer. These devices are frequency dependent, the ratios depending to some extent on winding impedance, core size, shut capacitance, etc. The ratio transformer was designed for 400 Hz operation but we would like to work at a higher frequency and had intended to use 1592 Hz ($\omega = 10^4$), the frequency of our research bridge. The NBS Electrical Measurements Section has determined the accuracy of the ratio transformer as a function of frequency to establish the size of the errors involved; the results are shown in Fig. 13. Ratio settings of 0.2, 0.5, and 0.8 are plotted versus frequency squared. Theoretically, errors in ratio settings reach maxima at the 0.8 settings plotted in the figure.

We decided to operate the bridge at 1,000 Hz where the accuracy of all ratios is within $2:10^7$, and, in addition, the ratios all err in the same way except for the two lowest settings. We have tested the bridge to a limited extent in our laboratory and believe it to be measuring with a precision approaching $1:10^7$. The bridge has been shipped to Redstone Arsenal for further testing which will include an evaluation of the effects of temperature, humidity, and vibration.

The bridge circuits are completely documented in a way which should facilitate their reproduction. Complete blue prints have been maintained and, in addition, wiring locations have been put on punch cards. Print-outs of different sorting sequences of the cards have been valuable aids in both the original wiring and in trouble-shooting.

The basic design and construction of this capacitance bridge has been primarily due to the efforts of Robert S. Kaeser of this laboratory.

CURRENT DEVELOPMENTS

We are continuing to look at any material we can acquire in order to get more capacitance data and possibly find other useful transducer materials. As mentioned above, we are continuing to look at samples of BGO in the hope that the observed instabilities may be only sample dependent. Since the resolution of capacitive transducer is essentially independent of pressure it is ideal for measurements at high pressures. For this reason we are extending our experiments to 700 MPa (100,000psi) to see how the capacitance gauge will operate in that range. At these higher pressures piston gauges become less accurate because of fluid viscosity problems. These problems should not effect the capacitive transducer so there should be little trouble achieving potential accuracies in excess of that of the piston gauges. We see no reason why the calcite pair combination can not be used to these higher pressures since it does not undergo any phase transitions until 1.4 GPa (200,000psi).

APPENDIX

Cooling of a Pressure Vessel upon Pressurization

The isothermal heating which occurs in piece of material under compressive stress can be calculated by writing the formula (see M. W. Zemansky, Heat and Thermodynamics, 5th Ed., p.288)

$$Q = - T \int V \beta \, dP \quad (A1)$$

Where β is the volume thermal expansion. This can be written in a more general form as

$$Q = - T \iiint \alpha \, dS \, dV. \quad (A2)$$

$dS = \Sigma dS_i$ is the sum of the three components of the stress acting on the volume dV . $\alpha = 1/3 \beta$ is the linear thermal expansion coefficient. Shear stresses are neglected.

The individual stress components for uniformly shaped pressure vessels under internal pressure, P , can be calculated using standard formulae as given by R. J. Roark (Formulas for Stress and Strain, 4th Ed., p. 308).

As a practical example we consider a cylindrical vessel with spherical ends. The internal and external radii are a and b and the stresses at a point r in the vessel wall are given by:

Cylindrical Portion -

longitudinal stress

$$dS_1 = \frac{a^2}{b^2 - a^2} dP,$$

hoop stress

$$dS = - \frac{a^2(b^2+r^2)}{r^2(b^2-a^2)} dP,$$

radial stress

$$dS_3 = + \frac{a^2(b^2-r^2)}{r^2(b^2-a^2)} dP,$$

Spherical Ends -

hoop stresses

$$dS_1 = dS_2 = - \frac{a^3(b^3+2r^3)}{2r^3(b^3-a^3)} dP,$$

radial stress

$$dS_1 = + \frac{a^3(b^3-r^3)}{r^3(b^3-a^3)} dP.$$

The contributions of the individual stress components can be found by multiplying by the appropriate volume element, $2\pi r dr$ for cylindrical segments and $4\pi r^2 dr$ for spherical segments, and integrating over r from a to b .

The total contribution is, however, more easily found since the sum of the three components of both segments are independent of r ,

$$dS_{cyl} = - 3 \left(\frac{a^2}{b^2-a^2} \right) dP$$

and

$$dS_{sph} = - 3 \left(\frac{a^3}{b^3-a^3} \right) dP \quad (A3)$$

The volume integrations of Eq. A2 can now be carried out separately giving

$$V_{cyl} = \pi l (b^2 - a^2)$$

and

$$V_{sph} = 4/3 \pi (b^3 - a^3) \quad (A4)$$

Multiplying the appropriate parts of Eqs. A3 and A4 and substituting in Eq. A2 we have

$$Q = T \int 3 \alpha (\pi a^2 l + 4/3 \pi a^3) dP$$

The expression in parentheses is just the internal volume V_i of the vessel so we can write

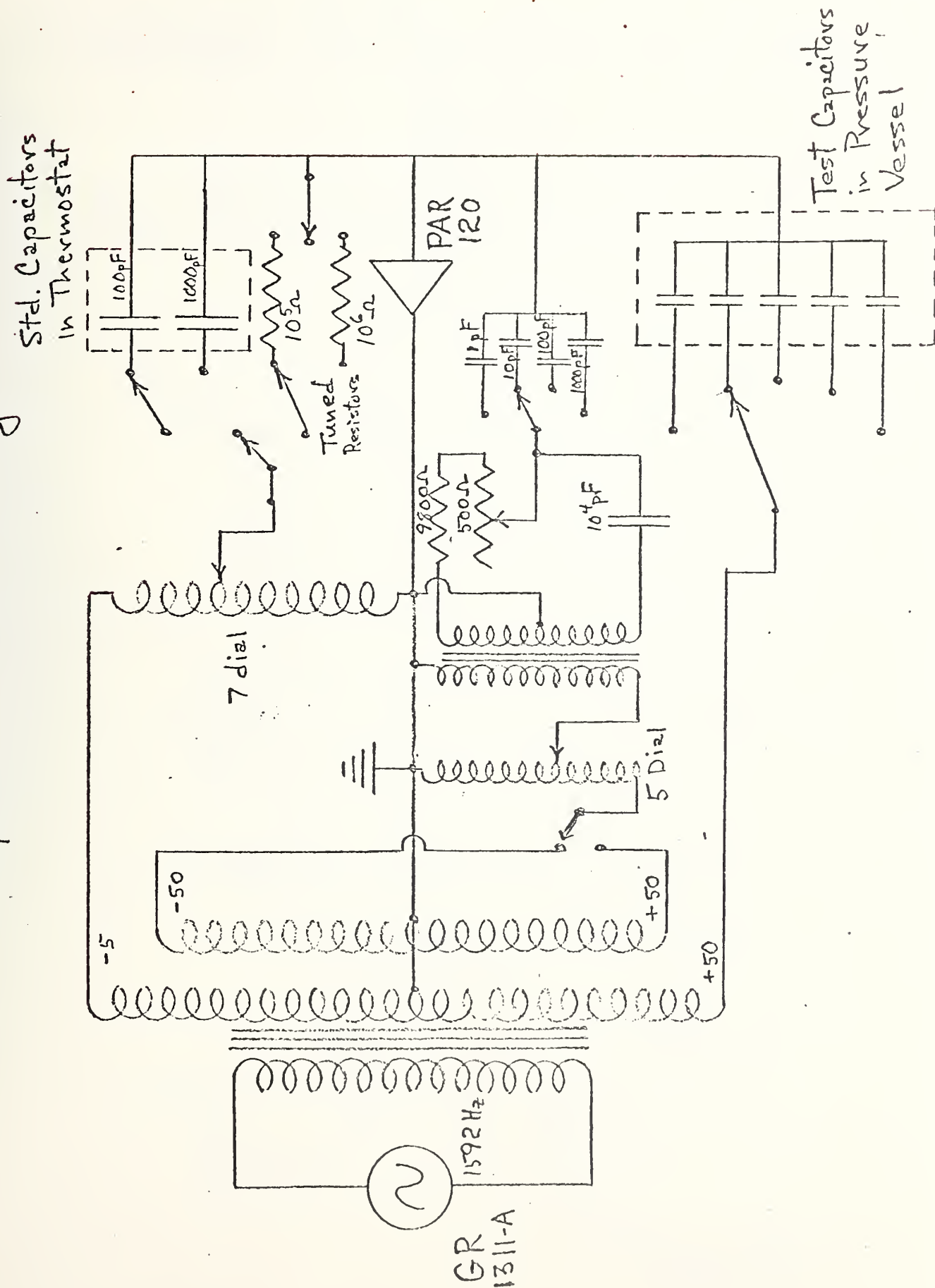
$$Q = T \int \beta V_i dP$$

This is just the expression for the compression heating by the pressure change dP of a volume V_i with thermal expansion β as given by Eq. 1A but with the sign changed.

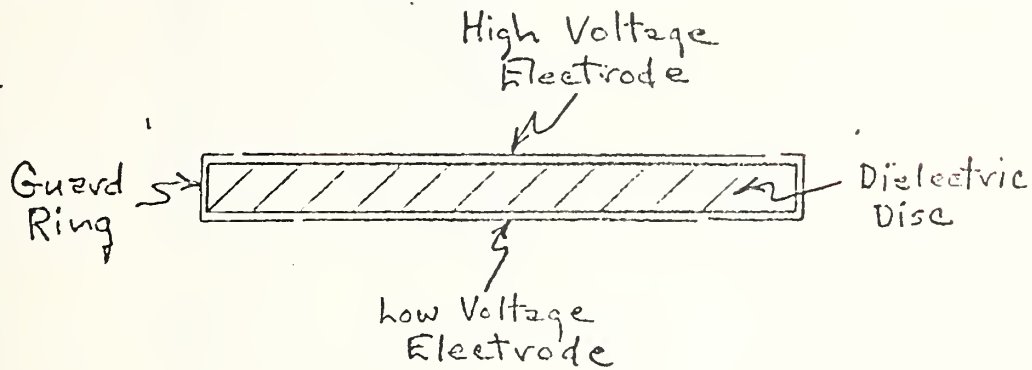
FIGURE CAPTIONS

- 1/ Capacitance Bridge.
- 2/ Electrode Configuration on Samples, Masking Rings, and Coating Arrangement.
- 3/ Sample Holder.
- 4/ Five Sample Holders Mounted on Pressure Vessel Closure.
- 5/ Pressure Dependence of a CaF_2 Capacitor at Four Temperatures.
- 6/ The Pressure Dependence of the Capacitance of Various Materials as a Function of Their Temperature Dependence. The temperature dependence is the atmospheric pressure value and the pressure dependence was determined at 35°C . The lines shown, join the values measured parallel and perpendicular to the crystalline axis of anisotropic materials and represent temperature and pressure dependences that could be realized for crystals cut at intermediate angles.
- 7/ Invar Sample Holder. The holder is shown assembled on the left and disassembled on the right. The holder is $1\frac{1}{2}$ inches in diameter and 6 inches long and fits snugly in the cavity of a commercial pressure vessel. The dielectric capacitors fit into recesses in the inner two plates and the electrical connections are made using small bellows as spring contacts.
- 8/ Invar Sample Holder and Pressure Vessel.
- 9/ Temperature changes at the outer surface of the isolated pressure vessel resulting from 140 MPa (20,000psi) pressure changes. The Vessel contains the Invar sample holder and about 5 cm^3 of pressurizing oil. The central peak is for decreasing the pressure to zero and the peak on the right is for repressurizing.
- 10/ Net temperature changes in the isolated transducer system as it is pressurized to 140 MPa (20,000psi) while containing different quantities of oil.
- 11/ Automatic Capacitance Bridge.
- 12/ Automatic Capacitance Comparator.
- 13/ Ratio errors as a function of frequency in programable ratio transformer.

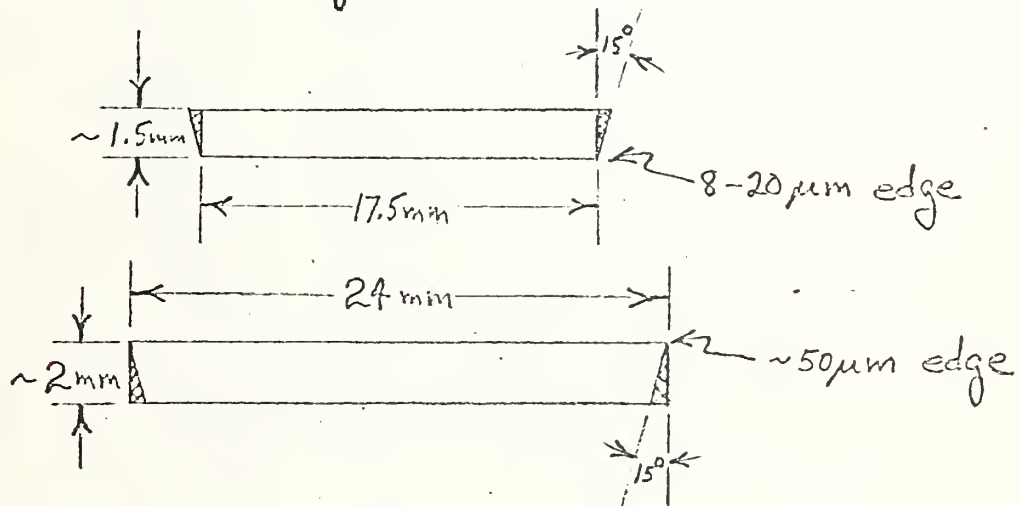
Capacitance Bridge



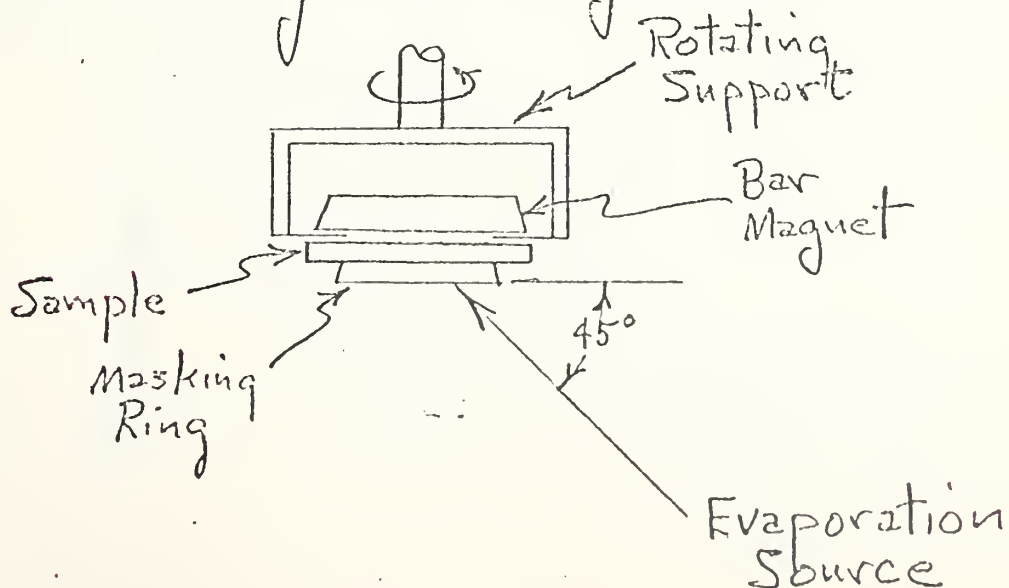
Electrode Configuration on Samples.



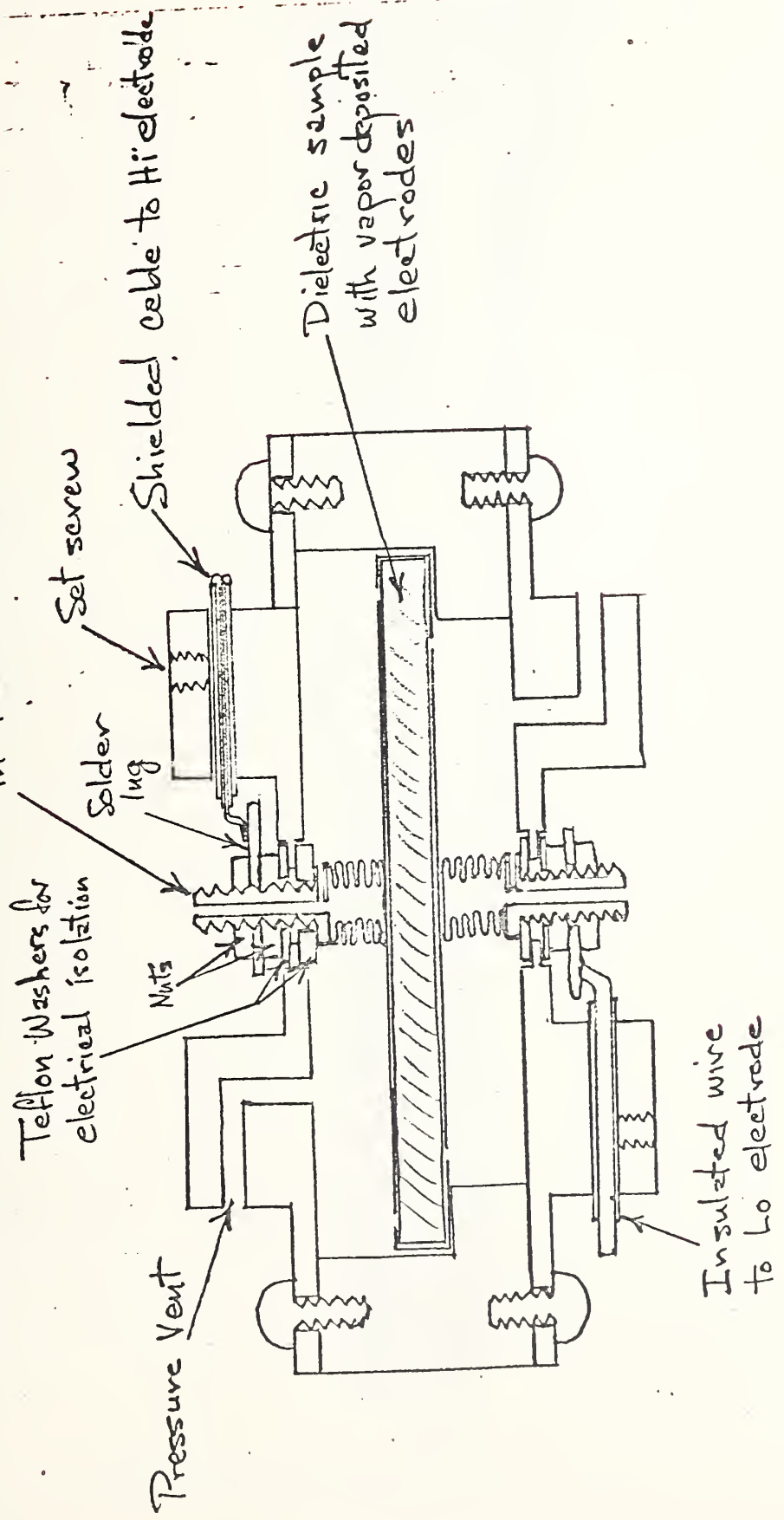
Masking Rings



Coating Arrangement



Electrical contacts consist of small nickel deposited bellows which are soldered to 4-40 screw studs. Holes through the screw studs allow pressure equalization in the bellows.



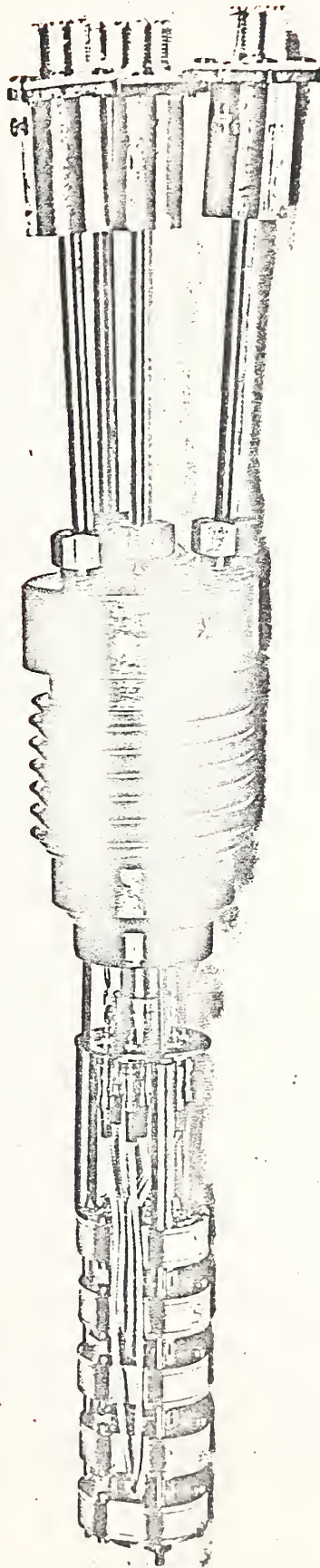


Fig 5

CaF₂

$\frac{\gamma}{\lambda} = 7000 \text{ Pa} = 1 \text{ psi}$

-36.5

-37.0

-37.5

-38.0

$\frac{\Delta C}{C_0 P} \times 10^{12} / \text{Pa}$

0

25

50

75

100

125

150

P (MPa)

5°C

20°C

35°C

50°C

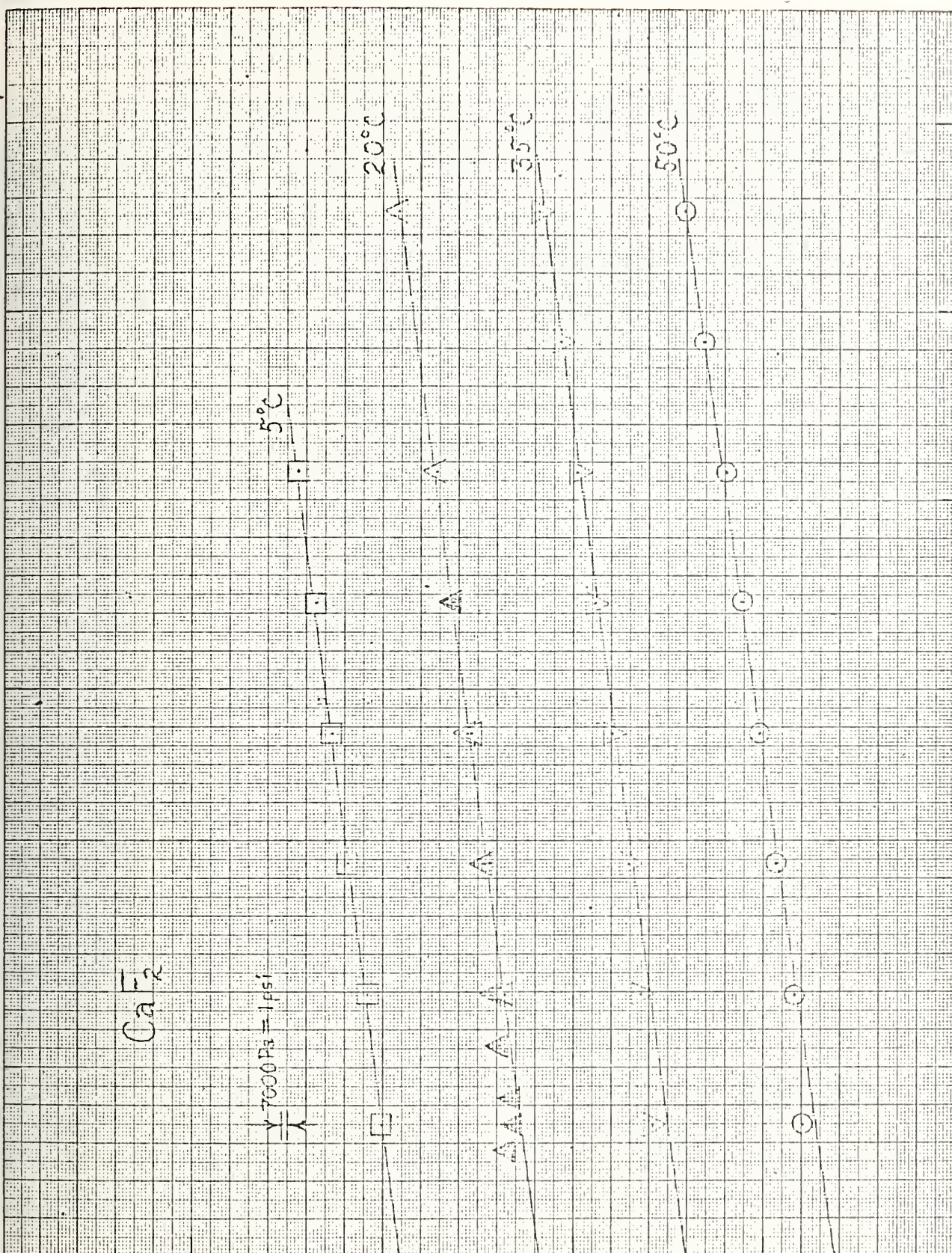


Fig. 6

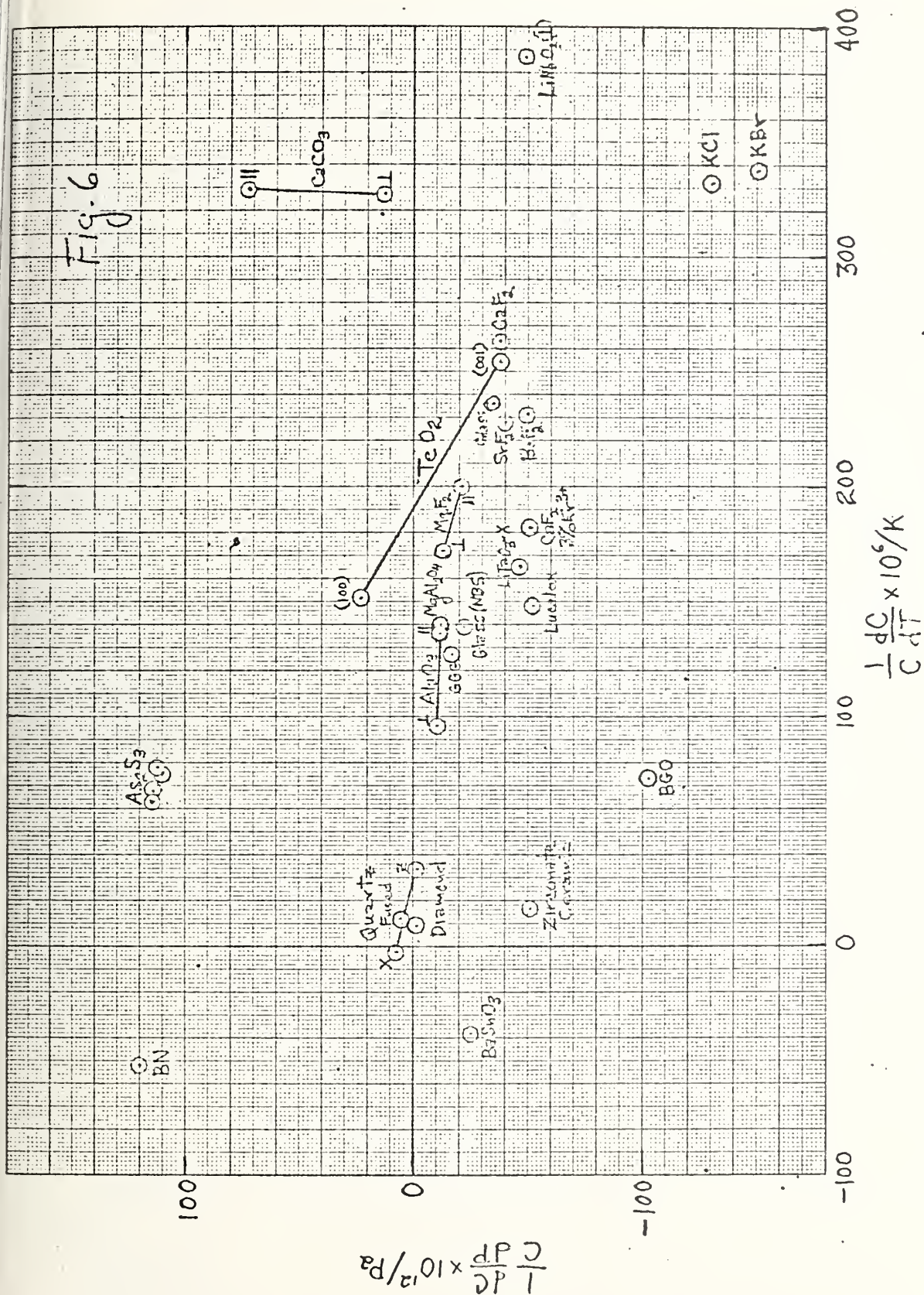


Fig. 7

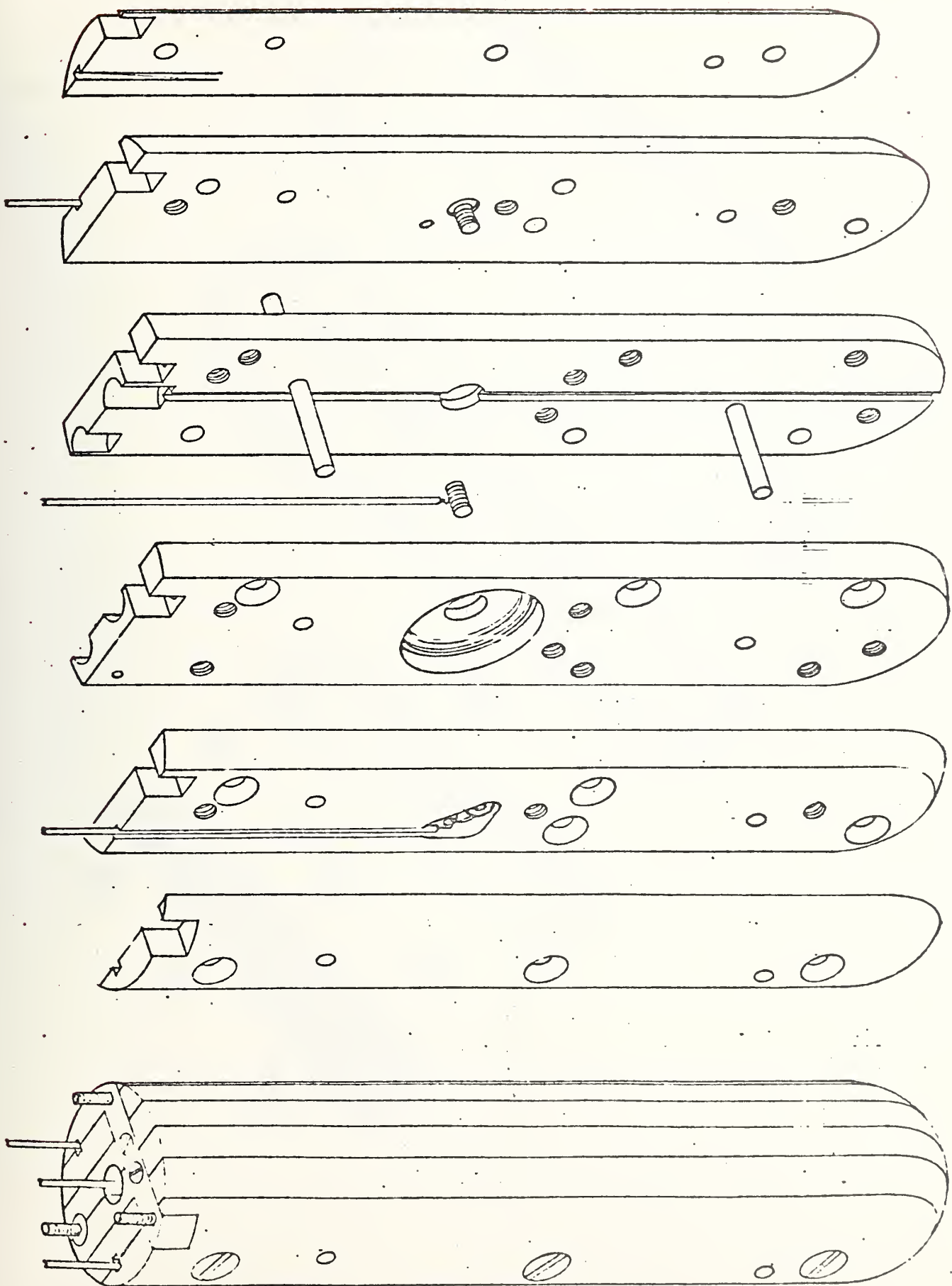
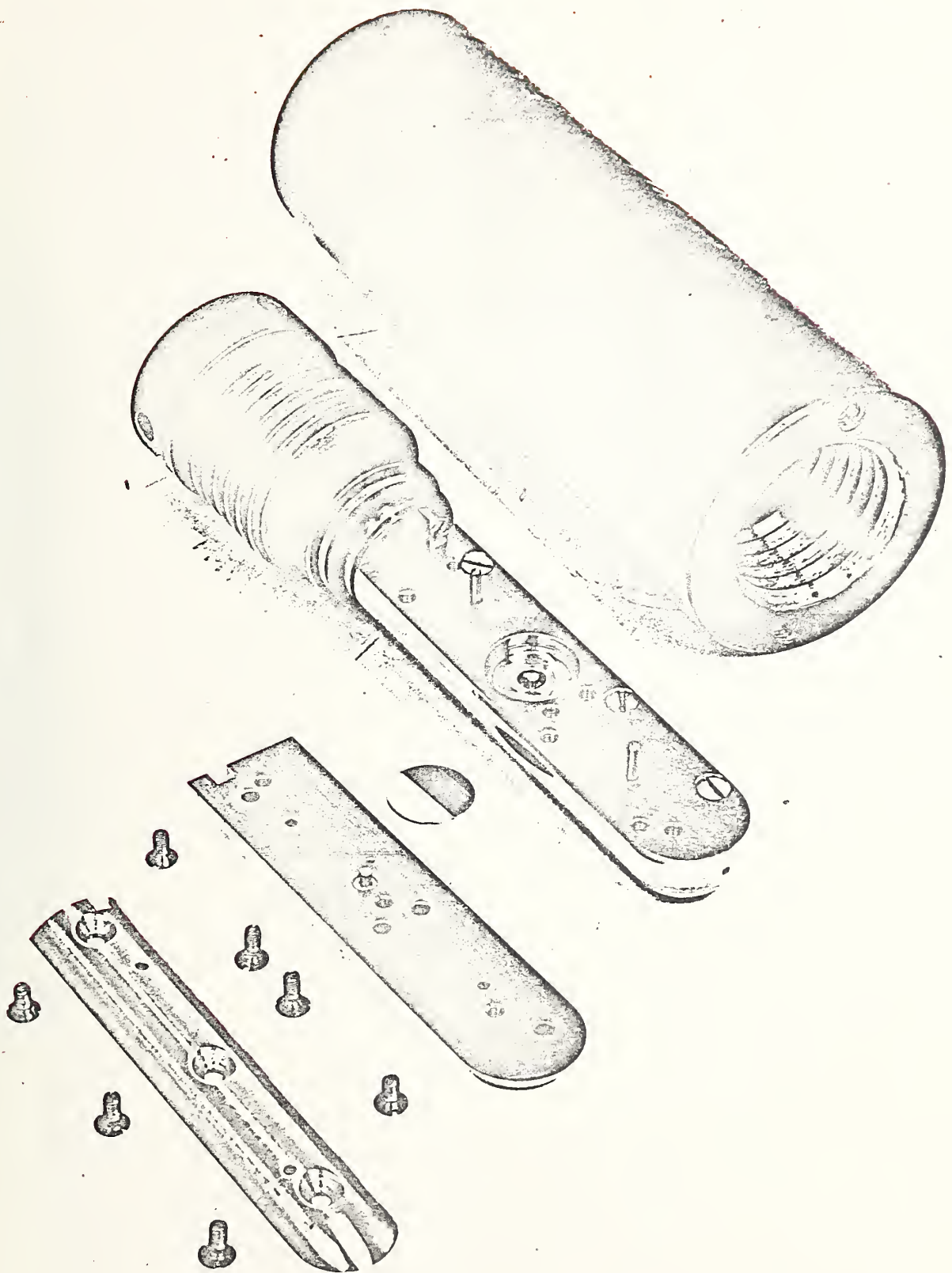


Fig. 8



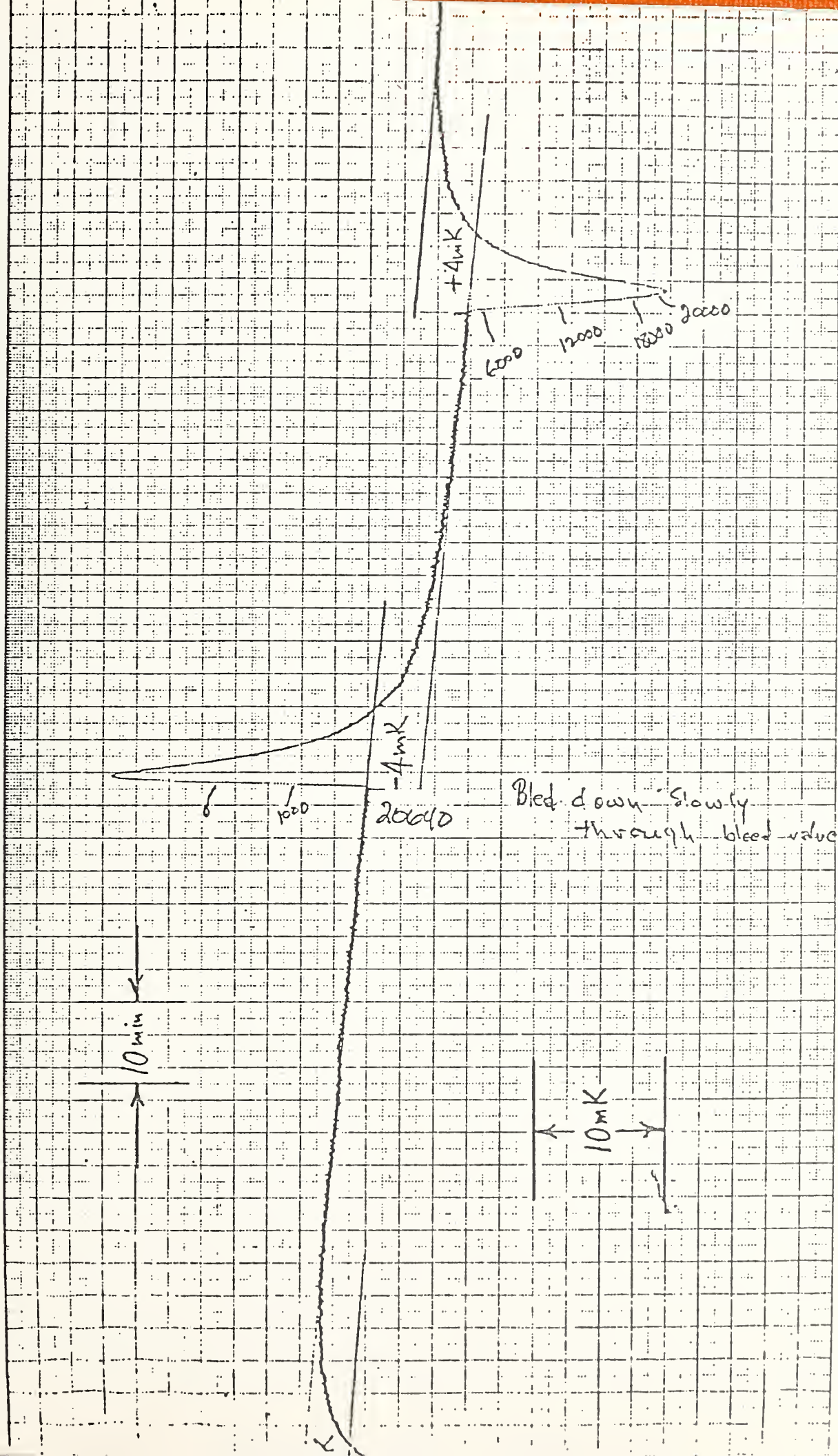
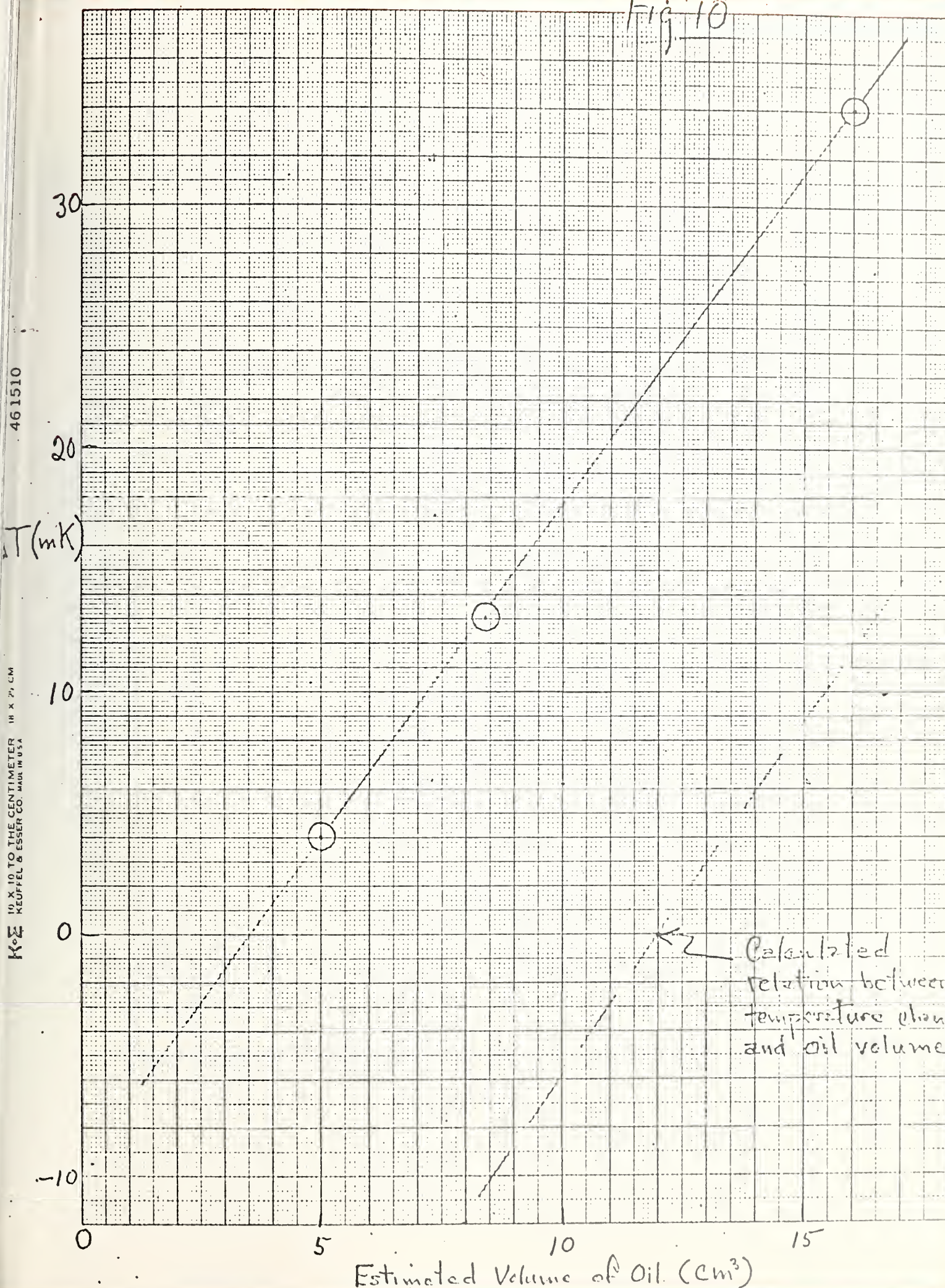


Fig 10

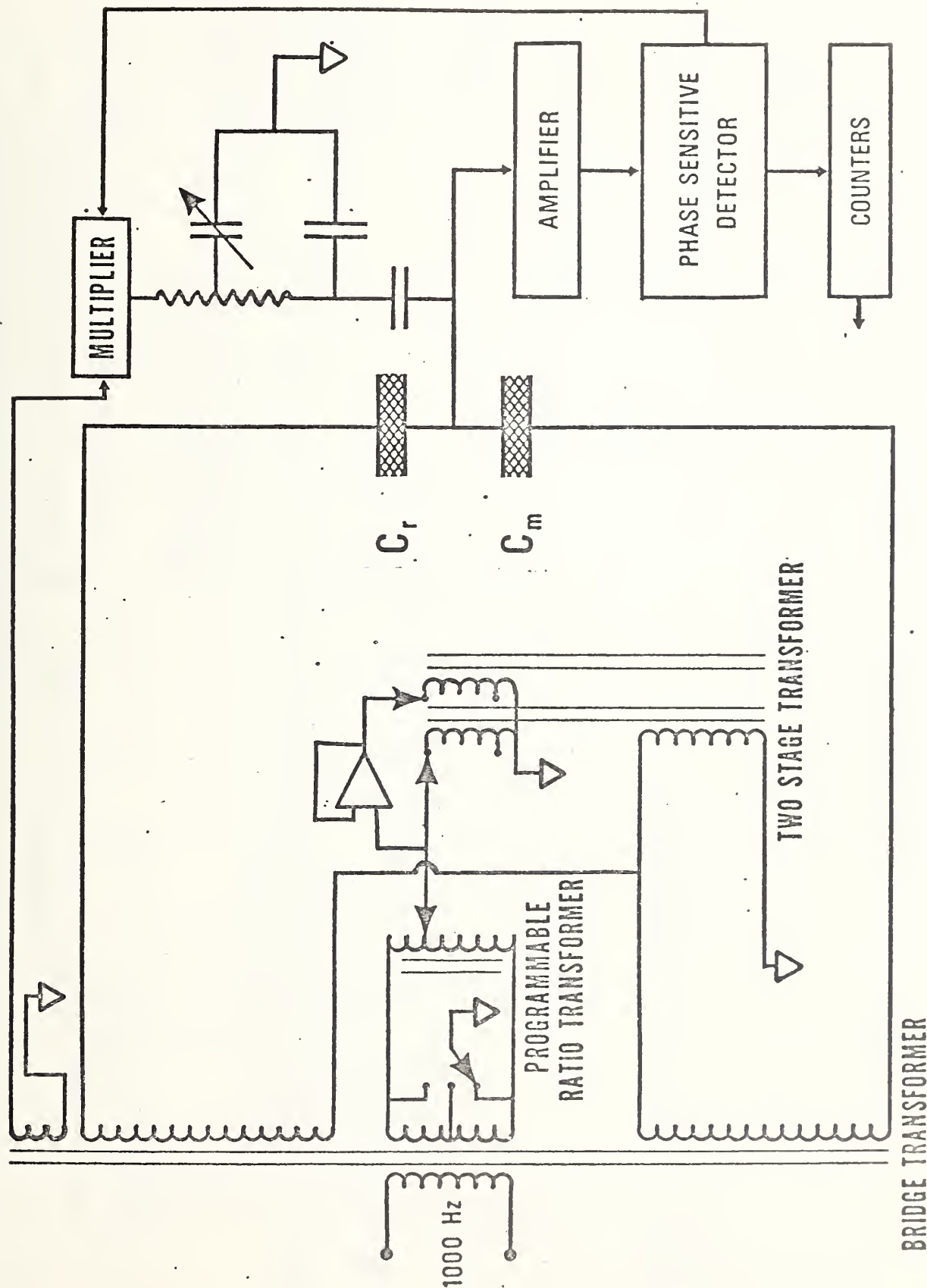
461510

K·Σ 10 X 10 TO THE CENTIMETER KEUFFEL & ESSER CO. MADE IN U.S.A.

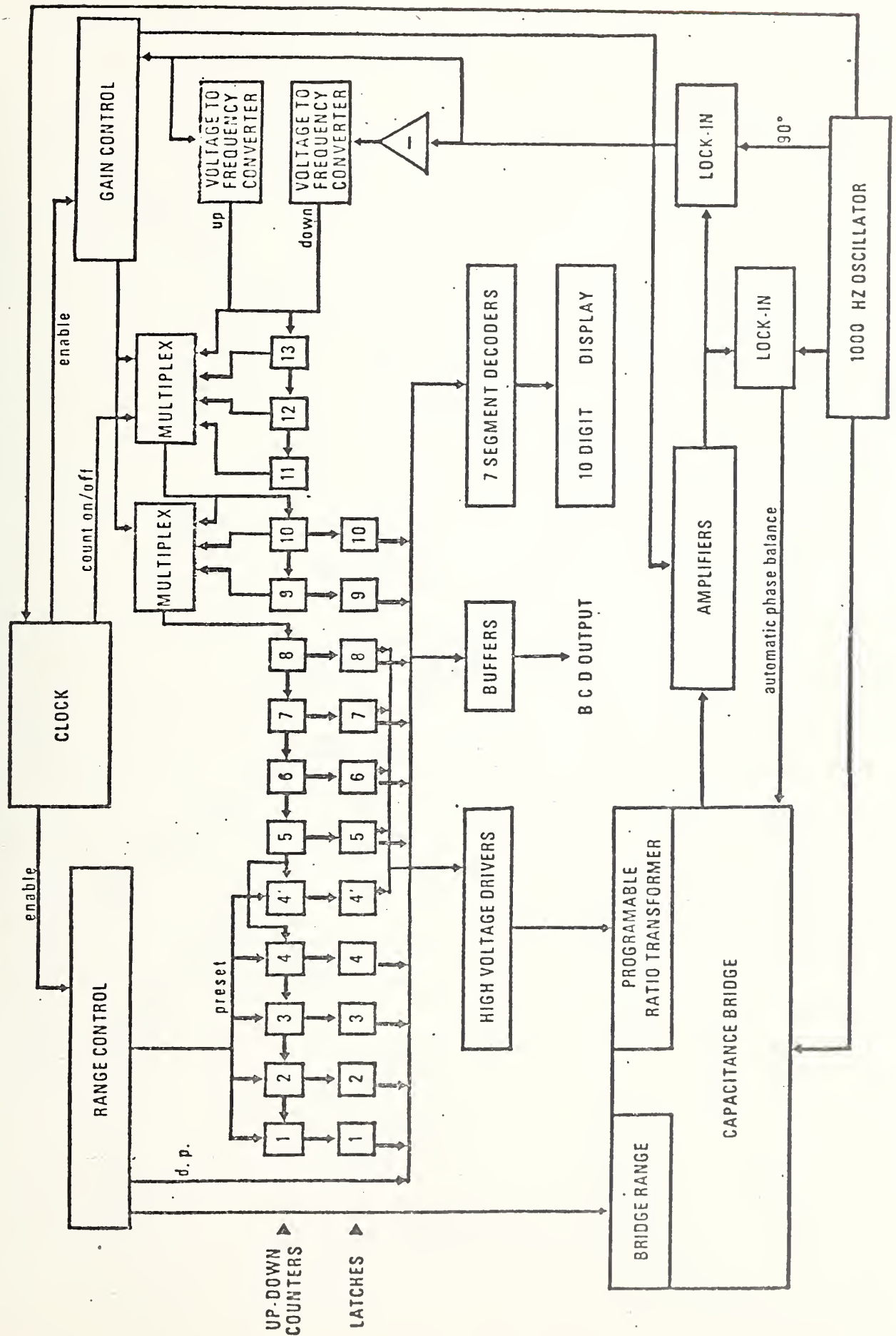


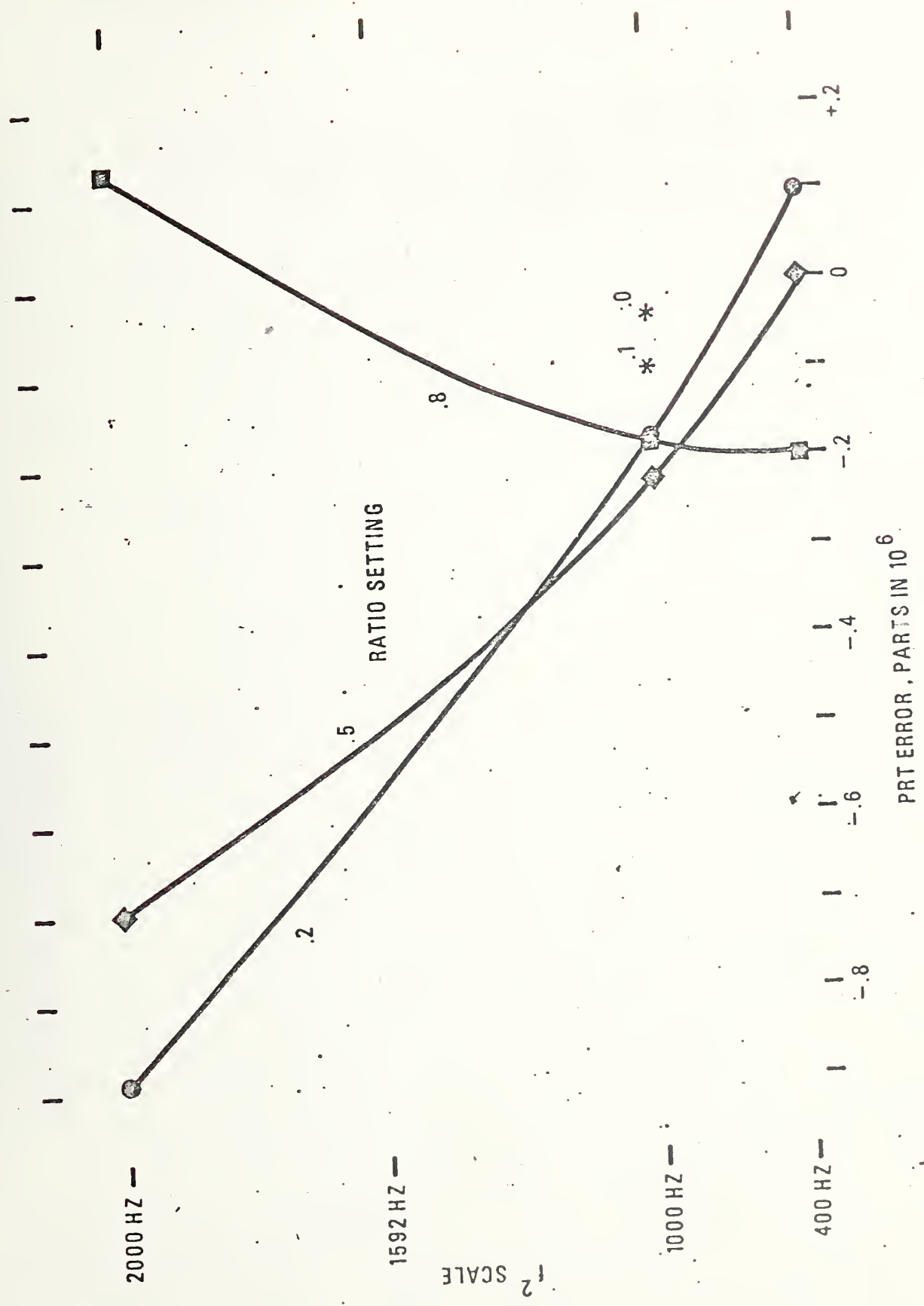
Calculated relation between temperature change and oil volume.

CAPACITANCE BRIDGE



AUTOMATIC CAPACITANCE COMPARATOR





SCALE f^2

